Siiman, O., Young, N. M., & Carey, P. R. (1974) *J. Am. Chem. Soc. 96*, 5583.
Solomon, I. (1955) *Phys. Rev. 99*, 559.
Solomon, I., & Bloembergen, N. (1956) *J. Chem. Phys. 25*, 261.
Solomon, E. I., Wang, R.-H., McMillin, D. R., & Gray, H. B. (1976) *Biochem. Biophys. Res. Commun. 69*, 1039.
Sternlicht, H. (1965) *J. Chem. Phys. 42*, 2250.
Tullius, T. D., Frank, P., & Hodgson, K. O. (1978) *Proc. Natl. Acad. Sci. U.S.A. 75*, 4069.
Vega, A. J., & Fiat, D. (1976) *Mol. Phys. 31*, 347.
Wherland, S., Farver, O., & Pecht, I. (1988) *J. Mol. Biol. 204*, 407.
Wüthrich, K. (1970) *Struct. Bonding 8*, 53–121.

X-ray Absorption Spectroscopy of the [2Fe-2S] Rieske Cluster in *Pseudomonas cepacia* Phthalate Dioxygenase. Determination of Core Dimensions and Iron Ligation†

Him-Tai Tsang,‡ Christopher J. Batie,§ David P. Ballou,*,§ and James E. Penner-Hahn*,‡
Department of Chemistry, University of Michigan, Ann Arbor, Michigan 48109-1055, and Department of Biological Chemistry, University of Michigan, Ann Arbor, Michigan 48109-0606

Received December 27, 1988; Revised Manuscript Received May 19, 1989

ABSTRACT: We have employed X-ray absorption spectroscopy to obtain structural information about the Rieske Fe/S center in the phthalate dioxygenase (PDO) from *Pseudomonas cepacia*. Native PDO contains a dinuclear Rieske Fe/S center and an additional mononuclear Fe site. In order to study selectively the Fe/S cluster, we measured data for samples in which the mononuclear site was either depleted of metal or reconstituted with Co or Zn. Our results demonstrate that the iron environment in the Rieske cluster is structurally indistinguishable from that found in other Fe/S clusters, thus strongly supporting the suggestion that the unusually high reduction potentials for Rieske clusters are due to electrostatic rather than structural effects. The average Fe–Fe distance is 2.68 (3) Å for both oxidized and reduced Rieske clusters. The average Fe–S distance is 2.24 (2) Å in the oxidized cluster and 2.28 (2) Å in the reduced cluster. Careful analysis of the EXAFS Debye–Waller factors suggests that the bridging and terminal Fe–S distances for the oxidized cluster are 2.20 and 2.31 Å, respectively. Taken together with recent ENDOR results, these studies provide a detailed structural model for the Rieske [2Fe-2S] centers.

Phthalate dioxygenase (PDO) is a stable protein that can be isolated in sufficient quantities for detailed structural characterization (Batie et al., 1987). In analogy to other such oxygenases, it catalyzes the first step in the metabolism of an unactivated aromatic compound, in this case phthalate, yielding the 4,5-*cis*-dihydrodiol of phthalate.

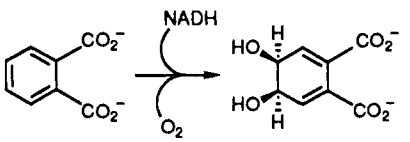

(1)

There are four identical subunits in PDO, each of which contains an Fe/S cluster that is spectroscopically indistinguishable from the "Rieske" Fe/S cluster (see below). In addition to the Fe/S cluster, ferrous ion is required for full activity (Batie et al., 1987). If the enzyme is dialyzed against EDTA to completely remove the ferrous ion, 1 equiv of Fe^{2+} must be added to reactivate the enzyme. Although other divalent metal ions will bind in place of Fe^{2+}, none will restore activity. The ferrous (mononuclear) site, which is >10 Å from the Rieske center (C. J. Batie, W. R. Dunham, and D. P. Ballou, unpublished work), has been proposed as the site of oxygen activation (Batie et al., 1987). We have employed EXAFS spectroscopy to obtain structural information about the Rieske center and to characterize the structural differences between Rieske clusters and the plant-type ferredoxins.

The Rieske-type cluster was first discovered (Rieske et al., 1964) in the mitochondrial ubiquinol–cytochrome *c* reductase system and was recognized by its unusual EPR spectral properties. Rieske clusters have since been found in photosynthetic electron-transfer proteins (Nelson & Newmann, 1972; Hurt & Hauska, 1981), in bacterial respiratory chains (Bowyer & Crofts, 1981; Gabellini et al., 1982), and in several bacterial oxygenases (Geary et al., 1984; Axcell & Geary, 1972; Gibson et al., 1970; Sauber et al., 1977; Batie & Ballou, 1987). The structure of the Rieske-type [2Fe-2S] center is of substantial interest because proteins containing this center have properties that are distinctively different from those of the ferredoxins. These properties include anomalous EPR, visible, and CD spectra and unusually high reduction potentials (−150 to 150 mV) [Kuila & Fee (1986) and references cited therein].

Characterization of the structure of the Rieske-type cluster is one important step toward understanding its properties. The Rieske cluster is believed to contain an Fe_2S_2 core similar to that found in the plant-type ferredoxins; however, in contrast to the ferredoxins, which have four symmetrically placed cysteine sulfurs surrounding the [2Fe-2S] core of the center,

†This work was supported by the National Institutes of Health, Grants GM38047 (J.E.P.-H.) and GM20877 (D.P.B.), and the Camille and Henry Dreyfus Foundation (J.E.P.-H.). X-ray absorption measurements were made at the Stanford Synchrotron Radiation Laboratory, which is supported by the U.S. Department of Energy and the National Institutes of Health.
*Authors to whom correspondence should be addressed.
‡Department of Chemistry.
§Department of Biological Chemistry.

0006-2960/89/0428-7233$01.50/0

the amino acid composition of the Rieske protein from *Thermus thermophilus* permits at most two thiolate ligands (Fee et al., 1984). Recent ENDOR spectroscopic studies of natural abundance (Cline et al., 1985) and of ^{15}N-enriched (Gurbiel et al., 1989) phthalate dioxygenase have now provided definite proof for ligation by two histidines in addition to the two cysteine residues. We report herein the results of an X-ray absorption study of the Rieske-type cluster found in phthalate dioxygenase, undertaken to permit direct comparisons between the structure of the Rieske center and those previously determined for rubredoxins, $Fe(SR)_4$ (Shulman et al., 1975, 1978; Sayers et al., 1976; Bunker & Stern, 1977; Watenpaugh et al., 1980), plant-type ferredoxins, $Fe_2S_2(SR)_4$, clostridial ferredoxins and high-potential iron–sulfur proteins, $Fe_4S_4(SR)_4$ (Tsukihara et al., 1978; Teo et al., 1979; Teo & Shulman, 1982), and the recently discovered 3Fe clusters (Antonio et al., 1982; Beinert et al., 1983; Stephens et al., 1985). The present work, together with recent ENDOR results (Gurbiel et al., 1989), substantially describes the structure of the Rieske Fe/S center.

Experimental Procedures

Sample Preparation. Phthalate dioxygenase was purified as previously described (Batie et al., 1987) with the exception that DEAE-agarose (Pharmacia) was used for both anion-exchange chromatographic steps. All samples were prepared in buffer A (100 mM HEPES/KOH, pH 8.0). Phthalate, if present, was at 5 mM. PDO was concentrated by ultrafiltration in centrifugal cells (Amicon Centricon 30). Reduced samples were prepared by addition of an excess of dithionite (ca. 10 mM) to the samples.

The native enzyme was depleted of its complement of mononuclear iron by dialysis at room temperature vs buffer B (50 mM HEPES, pH 8.0, 5 mM EDTA) + 1 mM $K_3Fe(CN)_6$. The apoenzyme, which still retains its Rieske center, was then equilibrated with buffer A by gel filtration. Zn-reconstituted PDO was prepared by adding 1 molar equiv of zinc acetate to concentrated apoenzyme.

Fully reconstituted PDO was prepared by adding 1 molar equiv of Fe(II) as a solution of ferrous ammonium sulfate to the enzyme. The enzyme–Fe(II) mixture was incubated for 5 min, EDTA (10 mM final concentration) was added, and the sample was incubated for a further 5 min. The enzyme was then separated from free $Fe^{II}EDTA$ and equilibrated with buffer A by gel filtration on Sephadex G-25 (Pharamacia).

XAS Measurements. X-ray absorption data were measured at the Stanford Synchrotron Radiation Laboratory by using a wiggler beam line (VII-3) equipped with a Si(220) double-crystal monochromator under dedicated conditions (3.0 GeV, ca. 50 mA, 18-kG wiggler field). The monochromator crystals were detuned by 50% to decrease harmonic contamination. All data were measured at 10–15 K by using an Oxford Instruments cryostat. Enzyme concentrations were typically 3 mM in protein. Data were measured as fluorescence excitation spectra by using a large solid-angle ion chamber (Stern & Heald, 1979) with Ar fill gas as the X-ray fluorescence detector and a combination of Mn filters and Soller slits to decrease scatter. The incident and transmitted beams were measured by using N_2-filled ionization chambers.

Reduced proteins retained their characteristic EPR signal at the end of data collection, indicating that there was no significant X-ray-induced damage to the Rieske site. As an additional measure of sample integrity, we compared the XANES spectra measured for the first and last scan of each sample. No changes were observed over the course of data collection.

Energy calibration was accomplished by using an Fe foil as an internal standard and assigning the energy of the first inflection point of this spectrum as 7111.2 eV. Data reduction followed standard procedures for background removal and normalization to a Victoreen polynomial (MacGillavry & Rieck, 1985). Initial conversion to k space, $k = [(8\pi^2 m_e/h^2)(E - E_0)]^{1/2}$, used a threshold energy, E_0, of 7130 eV; however, this parameter was allowed to vary in some of the curve fitting analyses.

Data Analysis. The EXAFS data were fitted to eq 2 by using a nonlinear least-squares algorithm. In eq 2, N is the

$$\chi(k) = \sum_i \frac{N_i S_i(k)\, F_i(k)}{kR_i^2} \exp(2k^2\sigma_i^2) \sin [2kR_i + \varphi_i(k)] \quad (2)$$

number of scatterers at distance R from the absorber, S is a scale factor (optionally k dependent), σ is the root-mean-square variation in R, $F(k)$ and $\varphi(k)$ are the backscattering amplitude and phase, the subscripts i refer to the ith absorber–scatterer pair, and the sum is taken over all absorber–scatterer pairs. Both ab initio and empirical parameters were used to describe the EXAFS amplitude and phase. Ab initio parameters (Teo & Lee, 1979) were calibrated by using a modification of the FABM method (Teo et al., 1983). In this procedure, the EXAFS data for a structurally characterized model compound are fitted to eq 2 with a k-independent S, and R, σ, and E_0 are allowed to vary, while N is fixed at the crystallographic value. The values of S and E_0 determined in this manner were 0.38 and 6.8 for Fe–S and 0.50 and −10 for Fe–O. For Fe–Fe, values of 0.35 and 5.25 were taken from Lindahl et al. (1987). These S and E_0 values were held fixed in subsequent refinements of protein EXAFS data. Empirical parameters were determined by using a Fourier filtering procedure to isolate the EXAFS for a single shell, which was then decomposed into an amplitude and a phase. In terms of eq 2, the empirical amplitude function is $S(k)\cdot F(k)$ while the phase function includes both $\varphi(k)$ and any correction term due to an incorrect choice of E_0. The model compounds used for both ab initio and empirical analyses were $Fe(acac)_3$ measured at room temperature for Fe–O, $Fe(SPh)_4(NEt)_4$ measured at 65 K for Fe–S, and $Fe_2S_2(S_2\text{-}o\text{-xylyl})_2(NEt_4)_4$ measured at 137 K for Fe–Fe. The use of Fe–O to model Fe–N scattering results in apparent bond lengths that are ca. 0.023 Å too short. This correction factor has been included in the bond lengths given below.

Regardless of the source of the amplitude and phase parameters, fits to the protein EXAFS data used three variable parameters per shell: N, R, and σ^2. For ab initio parameters, the σ^2 values obtained by the curve fitting procedure give the mean-square variation in absorber–scatterer bond length, while for empirical parameters the quantity which is determined is actually $\Delta\sigma^2$, where $\Delta\sigma^2$ is the difference between σ^2 for the protein and σ^2 for the model. Since there are two iron atoms/protein, the *average* coordination numbers, N, must be either integral or half-integral. In analyzing the protein EXAFS data, the optimum R and σ^2 were determined for all reasonable values of N. In this way it was possible to determine the optimal value for N while retaining a minimum number of freely variable parameters. Identical structural parameters were obtained for empirical and theoretical parameters; however, the empirical parameters consistently gave better fits. The results in Table I are based on empirical parameters. Initial fits were performed on Fourier-filtered single shells (first shell, R = 0.9–2.1 Å; second shell, R = 2.1–3.0 Å). Subsequent fits utilizing the unfiltered data gave

Table I: Curve Fitting Results for Rieske-like Cluster[a]

	first shell				second shell	
	Fe–S		Fe–N[b]		Fe–Fe	
sample	R (Å)	$\Delta\sigma^2 \times 10^3$ (Å^2)	R (Å)	F[c]	R (Å)	$\Delta\sigma^2 \times 10^3$ (Å^2)
oxidized						
+phthalate	2.22	0.6		1.33		
	2.24	4.2	2.06	0.48	2.68	−2.4
+Zn + phthalate	2.22	1.0		1.08		
	2.24	2.8	2.04	0.50	2.69	−2.9
+Zn − phthalate	2.22	−0.1		1.02		
	2.23	1.8	2.05	0.43	2.68	−3.6
reduced						
+phthalate	2.26	2.0		1.24		
	2.28	4.7	2.08	0.45	2.67	−2.0
+Zn + phthalate	2.26	1.5		1.23		
	2.28	4.8	2.09	0.48	2.67	−2.0
+Co + phthalate	2.26	1.6		1.25		
	2.28	4.5	2.09	0.42	2.68	−2.9
+Co − phthalate	2.27	1.8		1.04		
	2.28	4.9	2.10	0.35	2.69	−4.1
uncertainties	0.03	1.0	0.04		0.025	1.0

[a] Results of three EXAFS fits are shown for each protein. For the first shell (Fe–S + Fe–N) results are given for fits using either 3S only or 3S + 1N. For the second shell, results are given for fits using 1Fe. Inclusion of a shell of carbons at ca. 3.0 Å gives a modest improvement in the second-shell fit but no change in the Fe–Fe distance. [b] For the Fe–N shell only the distance is shown since the correlation between σ and coordination number is so large (see text). [c] Fit index defined as $[(k^3\chi_{obs} - k^3\chi_{calc})^2/(N_{data} - N_{var})]^{1/2}$, where N_{data} and N_{var} are the number of data points and number of variables, respectively.

equivalent structural results, albeit with decreased sensitivity to the Fe–N contribution. The precisions of the refined values for R and σ^2 were estimated as the range over which the parameter could be varied without increasing the mean-square deviation between data and fit by more than a factor of 2.

For quantitative analysis of the XANES region, we used a normalization procedure (G. S. Waldo and J. E. Penner-Hahn, unpublished work) in which the data are corrected, by subtraction of a single low-order polynomial and by multiplication by a single scale factor, to give the best agreement both below and above the edge to tabulated X-ray absorption cross sections. The intensity of the 1s–3d transition was estimated by first fitting a background function (linear function + arctan) to the regions below (7100–7109 eV) and above (7115–7120 eV) the 1s–3d transition. This background was then subtracted from the data to give the isolated 1s–3d peak. The area of this peak was determined by numerical integration. Equivalent results were obtained by fitting the entire preedge region (7100–7120 eV) by using a sum of linear + arctan + Gaussian functions.

Results and Discussion

EXAFS Spectra. The Fe EXAFS spectra for native PDO contain information about both the Rieske and the mononuclear Fe sites and are consequently difficult to interpret. In order to study specifically the Rieske cluster, it was necessary to make measurements on samples in which the mononuclear Fe had been removed. We have studied both samples in which the mononuclear site is vacant (2Fe proteins) and samples in which Zn or Co has been added to the mononuclear site (2Fe + M, M = Zn, Co). We have measured spectra for samples having either oxidized or reduced Rieske clusters. Most samples were studied in the presence of phthalate; however, two samples were also studied in the absence of phthalate. This set of samples allows us to determine the structural consequences of the oxidation state of the Rieske site, the presence of metal in the mononuclear site, and the binding of substrate. The specific samples studied are listed in Table I.

Fe EXAFS spectra for the samples in Table I are shown in Figure 1. The obvious beat pattern in these data reflects the fact that there are at least two shells of scatterers (i.e., sulfur and iron) making significant contributions to each EXAFS spectrum. It is obvious from a simple comparison of the EXAFS spectra for the oxidized and reduced Rieske clusters that the cluster undergoes some sort of structural rearrangement on reduction (this is especially obvious in the k = 6–9 Å^{-1} region).

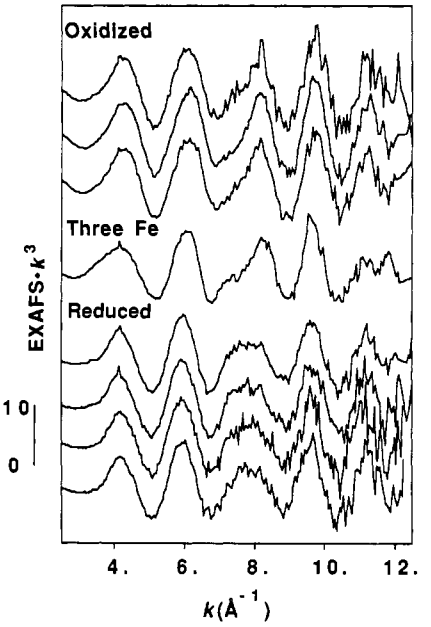

FIGURE 1: EXAFS spectra for oxidized and reduced Rieske clusters in phthalate dioxygenase. All spectra have been weighted by k^3 to enhance the EXAFS oscillations. From top: Oxidized 2Fe protein + phthalate; oxidized + Zn − phthalate; oxidized + Zn + phthalate; oxidized 3Fe protein + phthalate; reduced 2Fe protein + phthalate; reduced + Zn + phthalate; reduced + Co − phthalate; reduced + Co + phthalate. Spectra are plotted on the same scale and displaced vertically for clarity. Vertical scale is indicated by bar on left.

The EXAFS spectrum for the oxidized 3Fe protein is very similar to, although not identical with, those for the oxidized 2Fe proteins. This demonstrates that the EXAFS oscillations from the mononuclear iron are weak in comparison with those from the Rieske cluster, suggesting that the mononuclear site has predominantly low-Z ligands (oxygen or nitrogen) since

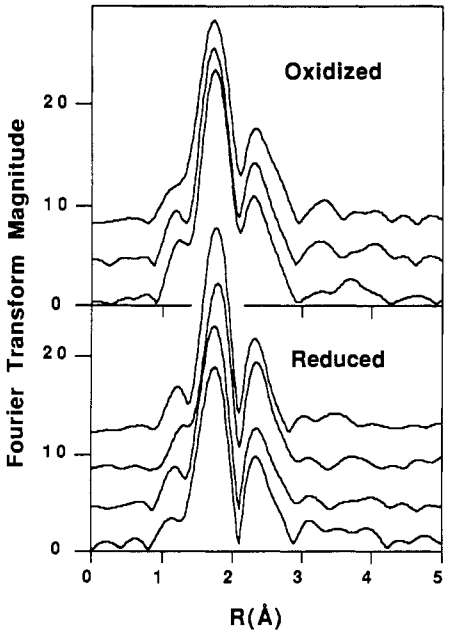

FIGURE 2: Fourier transform for Fe EXAFS for phthalate dioxygenase derivatives that have been depleted in mononuclear Fe. The two peaks correspond (primarily) to Fe–S and Fe–Fe scattering. In addition to a small shift in Fe–S distance on reduction, there is a characteristic change in shape of the second shell between oxidized and reduced centers. From top: Oxidized + Zn + phthalate; oxidized 2Fe protein + phthalate; oxidized + Zn – phthalate; reduced + Co + phthalate; reduced + Co – phthalate; reduced 2Fe protein + phthalate; reduced + Zn + phthalate. Spectra are plotted on the same scale and displaced vertically for clarity.

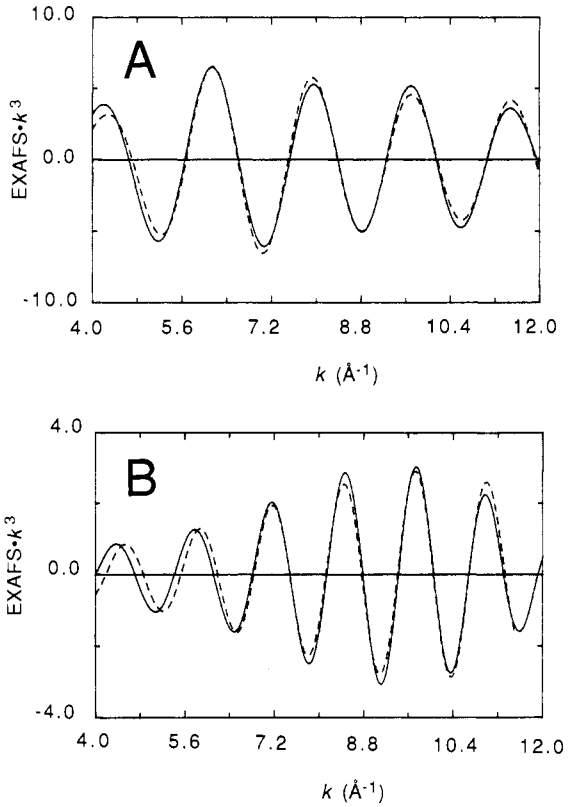

FIGURE 3: Representative fits of filtered Rieske-site EXAFS data. Fits to data for oxidized 2Fe protein + phthalate. Solid line = filtered experimental data; dashed line = best fit. Best fit parameters given in Table I. (A) First shell data (filter range = 0.9–2.1 Å) fit with S + N. (B) Second-shell data (filter range = 2.1–3.0 Å) fit with Fe + C.

these are weak scatterers in comparison with sulfur and iron. Given this situation, it is difficult to extract accurate structural parameters for the mononuclear site from the EXAFS of the 3Fe protein, and this sample will not be discussed further. A detailed structural characterization of the mononuclear site, based on Zn and Co EXAFS for Zn- and Co-substituted PDO, will be described in a subsequent publication.

The Fourier transform of an EXAFS spectrum has peaks corresponding to each of the different shells of scatterers, with the peak positions shifted by α (typically –0.4 to –0.5 Å) from the true absorber–scatterer distance (Sayers et al., 1971). The Fourier transforms of the PDO EXAFS data (Figure 2) show two peaks at $R + \alpha = 1.8$ and 2.2 Å, corresponding to Fe–S and Fe–Fe scattering, respectively. The Fe–N scattering, which must be present given the ENDOR results (Gurbiel et al., 1989), is not resolved from the first-shell Fe–S EXAFS.

In apparent contrast to Figure 1, the data in Figure 2 suggest that the changes in Rieske site structure on reduction are relatively minor. On close examination, the principal changes in the Fourier transforms appear to be a small shift in the position of the first shell and a change in the shape of the second-shell peak (note particularly the improved resolution of the Fe–S and Fe–Fe peaks for the reduced cluster relative to the oxidized cluster). The Fourier transforms clearly show that the cluster structure remains intact on reduction; the differences between oxidized and reduced EXAFS (Figure 1) reflect the sensitivity of the EXAFS beat pattern to small changes in bond length.

There are minor changes in the EPR spectrum of the Rieske-type cluster when the mononuclear Fe is removed (Batie et al., unpublished work). Addition of 1 equiv of a variety of divalent metals, including Fe(II), Co(II), and Zn(II), restores the Rieske-site EPR spectrum to that of the native protein. This suggests that there could be a structural rearrangement in the Rieske site depending on the occupation of the mononuclear site. Although there are minor variations among the Fourier transforms for oxidized Rieske clusters and among those for reduced Rieske clusters (Figure 2), these differences reflect the sensitivity of Fourier transforms to noise rather than real structural changes in the Rieske cluster. This is best illustrated by Figure 1, where it is clear that the different oxidized and the different reduced EXAFS spectra are identical within the noise level of the data. From this we conclude that occupation of the mononuclear site causes no detectable perturbations in either the oxidized or the reduced Rieske-site structures. These results will be described in more detail elsewhere (Batie et al., unpublished work). Likewise, the binding of phthalate has no detectable effect on the structure of the Rieske-like cluster.

Quantitative curve fitting analyses (Table I and Figure 3) support these conclusions. In general, the Rieske cluster has structural parameters consistent with those seen for other Fe/S clusters (Berg & Holm, 1982; Teo et al., 1979; Teo & Shulman, 1982; Antonio et al., 1982; Beinert et al., 1983; Stephens et al., 1985; McDermott et al., 1988). This finding, while not unexpected, is the first direct evidence that the unusually high redox potentials of Rieske-like clusters do not arise from gross structural changes in the Fe/S core and that this property must therefore derive from the replacement of two cysteine thiolates with histidine nitrogens. Reduction of the cluster results in a ca. 0.04-Å increase in the Fe–S distance. This is somewhat larger than the 0.02-Å increase observed for ferredoxin-like clusters (Teo et al., 1979), possibly reflecting the less polarizable nature of imidazole nitrogens as compared to cysteine sulfurs.

There appears to be a very slight decrease in the Fe–Fe distance (ca. 0.01 Å) on reduction. This difference is well

within the estimated uncertainty in bond length; however, the fact that the difference between oxidized and reduced clusters is reproduced across several samples suggests that it *may* be a real effect. A similar decrease was reported for the Fe–Fe distances in *Desulfovibrio gigas* ferredoxin (Antonio et al., 1982); however, for plant-type ferredoxins the Fe–Fe distance was reported to *increase* by 0.03 Å on reduction (Teo et al., 1979).

Given the ENDOR evidence that two histidine imidazoles are coordinated to the Rieske cluster (Gurbiel et al., 1989), there must be four carbons at ca. 3.0 Å from the irons and two carbons and two nitrogens at ca. 3.4 Å. The former will contribute to the 2.2-Å "Fe–Fe" peak in Figure 2; hence it is not surprising that fits to the filtered second-shell data are improved by ca. a factor of 2 on inclusion of a shell of carbon. The best fits are obtained for $N_{Fe-C} = 1$. This deviation (expected value = 2C/Fe) may reflect disorder in the imidazole orientations (i.e., a range of Fe–C distances) or may simply reflect the difficulty of defining weak Fe–C scattering in the presence of strong Fe–Fe scattering. Support for the latter view is found in the fact that the Fe–C shell refines to two equally good minima with R_{Fe-C} ca. 2.74 and 3.01 Å, although only the longer of these is consistent with known Fe–imidazole structures. We conclude from this that it will be extremely difficult to reliably define the Fe–C interactions in the Rieske cluster and related systems and have for this reason omitted the Fe–C scattering from Table I. From Figure 2 it is clear that the third-shell C and N scatterers at ca. 3.4 Å make only minor contributions to the observed EXAFS; we have made no attempt to interpret their scattering quantitatively.

For Fe–S and Fe–Fe distances of ca. 2.25 and 2.7 Å, the calculated S–Fe–S and Fe–S–Fe angles are ca. 105° and 75°, with only minor (<5°) variations between oxidized and reduced clusters. However, in order for the Fe–S distances to increase while the Fe–Fe distance stays fixed or decreases slightly, there must be a substantial increase in S···S distance between oxidized and reduced clusters. The precise S···S distance is difficult to determine since the distances in Table I are an average over all Fe–S pairs. However, given the Fe_2S_2 core structure, the increase in S···S distance will, for a fixed Fe–Fe distance, be ca. 2.5 times larger than the increase in Fe–S distance. Thus, a reasonable estimate for the increase in S···S distance is 0.1 Å. This accordion type of motion on reduction is consistent with the notion that S···S repulsion plays an important role in determining the Fe_2S_2 core structure (Maelia & Koch, 1986).

One of the unique features of Rieske-like clusters is their nitrogen coordination. It is therefore somewhat disappointing that the Fe–N distance is only poorly defined by the EXAFS data. In initial fits, using uncalibrated plane-wave ab initio parameters, we were unable to show unambiguously that nitrogen was even present in the first coordination sphere (Penner-Hahn et al., 1987). This was due to the large number of parameters (N, R, E_0, S) and the ambiguity in the choice of scale factor in these fits. Subsequent fits using the procedures described above had fewer variable parameters and thus less severe parameter correlation problems. These fits (Table I) provide clear evidence for nitrogen coordination, in that the quality of fit improves at least 2-fold for two-shell vs one-shell fits. Even in this case, the nitrogen coordination remains poorly defined and it would be difficult on the basis of EXAFS alone to determine the number of coordinated nitrogens. Similar difficulties in defining low-Z ligation in the presence of sulfur ligation were encountered by Lindahl et al. (1987) in studies of 4Fe/4S clusters.

Several factors contribute to the poor definition of the Fe–N coordination number. The low scattering power of one nitrogen in comparison with three sulfurs and one iron limits the contribution of the nitrogens to the overall EXAFS spectrum. In addition, there is a strong correlation between coordination number and Debye–Waller factor. Finally, the sulfur and nitrogen coordination numbers are positively correlated since Fe–S and Fe–N EXAFS oscillations are approximately out of phase. This means that, within reason, an increase in the average nitrogen coordination number, N_N, can be compensated by an increase in the average sulfur coordination number, N_S.

Fortunately, we know a great deal about the expected coordination numbers and can use this information to restrict the number of variable parameters. For each of the samples, the best single-shell fit is obtained by using $N_S = 3$. From the ENDOR (Gurbiel et al., 1989), we expect N_N to be 1 and have used this for the two-shell fits in Table I, although comparable fits are obtained for larger values of N_N. Variation in N_N has little effect on R_S, σ_S, or R_N but results in significant changes in σ_N. Since the σ_N values are so poorly defined, they have been omitted from Table I.

The distances reported in Table I and the discussion thus far are based on average Fe–ligand bond lengths; however, detailed interpretation of the Fe_2S_2 core structure requires knowledge of the terminal thiolate (Fe–S_t) and bridging sulfide (Fe–S_b) bond lengths. Although this information is not directly available, it is possible to estimate the spread in distances from the magnitude of the Debye–Waller factors. The measured σ^2 values contain contributions from both static and dynamic (vibrational) disorder: $\sigma^2 = \sigma_{vib}^2 + \sigma_{stat}^2$. All of the Fe–S EXAFS data were measured at low temperatures [protein data at 10 K, $(Et_4N)Fe(SPh)_4$ at 65 K]. For typical Fe–S vibrational frequencies of ca. 300 cm^{-1}, these temperatures are sufficiently low that only the zero-point vibrational motion will contribute to σ_{vib}^2. Since the model and the protein should have similar zero-point Fe–S motion, the σ_{vib}^2 contributions should cancel and thus the experimentally determined $\Delta\sigma^2$ will be simply the change in σ_{stat}^2 between model and protein. Since the disorder in the model is negligible ($\sigma^2_{stat,model} = 1 \times 10^{-4}$; Koch et al., 1983), $\Delta\sigma^2$ should be a good approximation of the σ_{stat}^2 values for the protein.

Bridging and terminal Fe–S distances in [2Fe-2S] models generally differ by ca. 0.1 Å (Berg & Holm, 1982). In principle, all six Fe–S bond lengths in the Rieske cluster may be different; however, model studies (Coucouvanis et al., 1984) suggest that the chemical differences between the two irons are unlikely to lead to differences of greater than ca. 0.03 Å in the average bridging atom bond lengths for the different irons. It is possible that the sulfides may bridge the two irons asymmetrically; however, there are few examples of this (Coucouvanis et al., 1984). We have adopted an idealized model for the oxidized Rieske cluster in which there is one bridging bond length (Fe–S_b) and one terminal bond length (Fe–S_t). For this model

$$\sigma_{stat}^2 = [2(R_{Fe-S_b} - R_{av})^2 + (R_{Fe-S_t} - R_{av})^2]/3 \quad (3)$$

$$R_{av} = (2R_{Fe-S_b} + R_{Fe-S_t})/3 \quad (4)$$

since each iron is bonded to, on average, two bridging and one terminal sulfur. It is easy to show that, in general, the spread in bond lengths for oxidized Rieske clusters, $\Delta R = R_{Fe-S_b} - R_{Fe-S_t}$, is given by $3\sigma_{stat}(2^{-1/2})$. For $\sigma_{stat}^2 = (3 \pm 1) \times 10^{-3}$, this corresponds to $\Delta R = 0.09$–0.13 Å. Since $R_{av} = 2.24$ Å, this corresponds to $R_{Fe-S_b} = 2.20$ Å and $R_{Fe-S_t} = 2.32$ Å. This

Chart I

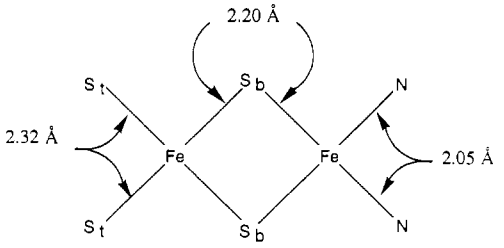

structure, which is illustrated schematically in Chart I, is in good agreement with the average bond lengths observed for crystallographically characterized Fe_2S_2 clusters (R_{Fe-S_b} = 2.20 Å, R_{Fe-S_t} = 2.31 Å) (Berg & Holm, 1982). These calculations confirm our earlier conclusion that the oxidized Rieske cluster is very similar structurally to other Fe_2S_2 clusters.

There is very little information available regarding the structures of reduced [2Fe-2S] clusters. No model compounds have been crystallized, and the only protein structures available come from EXAFS measurements (Teo et al., 1979; Teo & Shulman, 1982). The data in Table I show that the average Fe–S bond length increases and that there is a small increase in σ_{stat}^2 on reduction. In order to clarify the differences between oxidized and reduced forms of PDO, we have used the ratio-difference analysis procedure originally proposed by Sayers et al. (1974). In this procedure, one decomposes the filtered EXAFS data into an amplitude, $A(k)$, and a phase, $\varphi(k)$, where $\chi = A(k) \sin [\varphi(k)]$. For two single-shell compounds, labeled by subscripts 1 and 2, consideration of eq 2 shows that

$$\ln [A_1(k)/A_2(k)] = \ln (N_1/N_2) - 2k^2\Delta\sigma^2 \quad (5)$$

$$\varphi_1(k) - \varphi_2(k) = 2k\Delta R \quad (6)$$

Equations 5 and 6 are not strictly applicable to the Rieske-cluster data, since both sulfur and nitrogen contribute to the first-shell data. However, the contribution from nitrogen is weak and should, to a first approximation, cancel when comparing oxidized and reduced proteins. To the extent that cancellation is complete, plots of ln (A_{ox}/A_{red}) vs k^2 and $\varphi_{ox} - \varphi_{red}$ vs k should give straight lines with slopes corresponding to $-2\Delta\sigma_{ox\text{-}red}^2$ and $2\Delta R_{ox\text{-}red}$. Deviation of these plots from linearity will signal a breakdown of the simplifying single-shell hypothesis.

The data corresponding to eq 5 and 6, averaged over the two pairs of comparable oxidized and reduced proteins, are shown in Figure 4. For the first shell, the data are linear, giving parameters $\Delta\sigma_{ox\text{-}red}^2$ = [1.2 (5)] × 10^{-3} Å^2 and ΔR = 0.031 (5) Å. The estimated uncertainties in these values are smaller than the uncertainties given in Table I since many of the errors should cancel.

Interestingly, the ratio-difference data for the second shell are significantly nonlinear. This invalidates the single-shell hypothesis (eq 5 and 6); thus we cannot use this approach to estimate the changes in the Fe–Fe interaction. This result does, however, offer some insight into the Fourier transform differences observed in Figure 2. Although the second-shell peaks for oxidized and reduced proteins are qualitatively different, the results of the curve fitting analysis suggest that the dominant second-shell component (Fe–Fe) shows little change on reduction. The nonlinearity in Figure 4 is most likely due to incomplete cancellation of the contributions of non-(Fe–Fe) EXAFS. Typical Fe–C_{Cys} distances (3.4 Å) are too long to contribute to the second-shell peak; hence the most likely non-Fe candidates are the imidazole carbons at ca. 3 Å or another, as yet unidentified, ligand. A change in either of

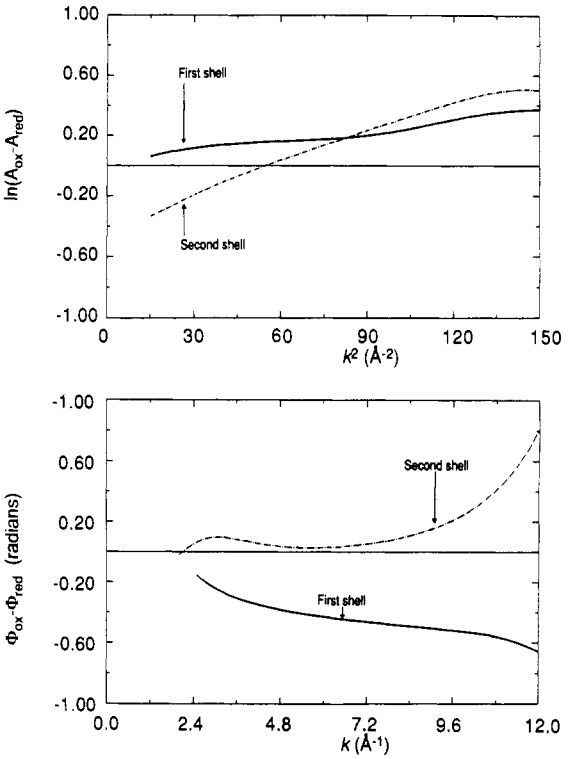

FIGURE 4: Amplitude-ratio (top) and phase-difference (bottom) plots for PDO calculated according to eq 5 and 6 in text. (Solid) First shell; (dashed) second shell. Ratios and differences were calculated for matched pairs of proteins: (oxidized 2Fe – reduced 2Fe), (oxidized 2Fe + Zn – reduced 2Fe + Zn). The plotted values are the average ratio and phase difference. The same E_0 was used for both oxidized and reduced proteins; however, variations in E_0 over ±20 eV were unable to reduce the curvature observed in the second-shell phase-difference plot.

these, i.e., rotation of an imidazole or addition of a new ligand, could account for both the nonlinearity in Figure 3 and the second-shell differences in Figure 2.

Detailed calculation of R_{Fe-S_b} and R_{Fe-S_t} is not possible for the reduced cluster, since there will be at least three different Fe–S distances. As a simplified model we start with the ENDOR result (Gurbiel et al., 1989) that two imidazoles are ligated to a single iron and the Mössbauer result that the reduced cluster is valence trapped (Fee et al., 1984), i.e., $N_2Fe_a(\mu\text{-}S)_2Fe_bS_2$. If all bond length changes are localized on the iron that is reduced, then the Fe(II)–S_b distances must increase by either 0.093 Å (if the imidazole-ligated iron, Fe_a, is reduced) or 0.046 Å (if Fe_b is reduced) in order to account for the observed increase in the average R_{Fe-S}. In model compounds, the observed increase in R_{Fe-S} on reduction of $Fe^{III}(SR)_4$ clusters is ca. 0.06–0.09 Å (Mayerle et al., 1975; Coucouvanis et al., 1976, 1981; Lane et al., 1977; Millar et al., 1982; Hagen et al., 1983; Jinxua et al., 1985), thus favoring the model in which Fe_a is the site of reduction. This is consistent with the intuitive notion that an iron which is ligated to two neutral imidazoles will be easier to reduce than an iron which is ligated to two anionic thiolates (Kassner & Yang, 1977). In this model, the calculated bond lengths are Fe(II)–S_b = 2.29 Å, Fe(III) – S_b = 2.20 Å, and Fe(III)–S_t = 2.31 Å. These Fe–S distances would give a decrease in static disorder relative to the oxidized cluster, in contrast to the observed *increase*; thus it appears likely that the reduced Rieske cluster is more disordered than suggested by our simple model.

It is important to emphasize that the preceding discussion gives our best estimate of the reduced Fe_2S_2 core structure,

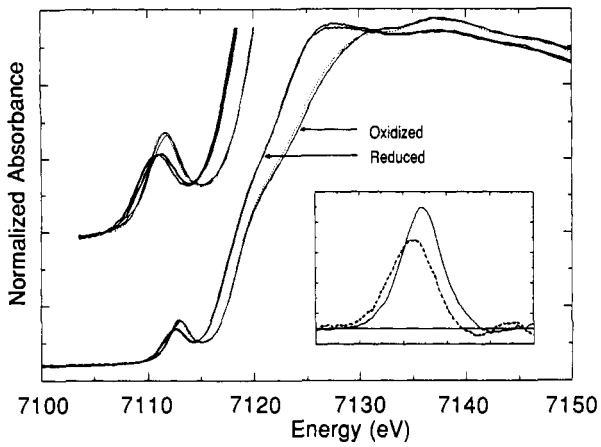

FIGURE 5: Representative XANES spectra for oxidized and reduced Rieske clusters. Inset shows isolated 1s–3d transition for oxidized (solid) and reduced (dashed) clusters.

within the context of the available information for the Rieske cluster. EXAFS does not, however, provide any *independent* evidence in favor of this model. Both $N_2Fe(III)(\mu\text{-}S)_2Fe(II)S_2$ and $SNFe(III)(\mu\text{-}S)_2Fe(II)NS$ models would also give bond lengths consistent with known Fe–S structures.

XANES Spectra. XANES spectra are sensitive to both oxidation state and geometry and thus provide a probe of the Rieske cluster which is complementary to EXAFS. The XANES spectra for PDO are shown in Figure 5. The shift of ca. 2 eV to lower energy on reduction is similar to that reported by Teo and co-workers (Teo et al., 1979; Teo & Shulman, 1982) for ferredoxins and is consistent with the presence of Fe(II). As was the case for the ferredoxins, we find that the reduced PDO edges show a more abrupt absorption discontinuity than the oxidized edges. McDermott et al. (1988) have suggested that such edge structure, at least for the ferredoxins, is indicative of oxidative decomposition. We see no evidence for such degradation in our samples.

Although XANES spectra are known to be sensitive to small changes in geometry, there does not exist at present a theory that is capable of giving an unambiguous interpretation of a particular spectrum in terms of molecular structure. Nevertheless, the fact that the edge shape is identical for the different oxidized and for the different reduced proteins suggests that there is no significant geometrical rearrangement when the mononuclear site is changed or when substrate is added, consistent with the EXAFS results.

The small feature on the low-energy side of the absorption edge is the 1s–3d transition. It is well-known that the intensity of the 1s–3d transition is sensitive to the geometry of the absorbing site, with very weak transitions being observed for centrosymmetric (e.g., octahedral) sites and relatively strong transitions being characteristic of tetrahedral coordination (Shulman et al., 1976). Roe et al. (1984) have shown that it is possible to correlate the Fe(III) 1s–3d intensity with coordination number. The normalized areas (in units of 10^{-2} eV) are 6–9 for 6-coordinate, 12–19 for 5-coordinate, and 23–25 for 4-coordinate Fe(III).

The 1s–3d transition for the Rieske cluster (inset to Figure 5) shows a significant decrease in intensity when the cluster is reduced. The normalized 1s–3d intensity for the oxidized cluster is 26, the same as that found by Roe et al. for 4-coordinate Fe centers, while the intensity for the reduced cluster decreases to 18. The observed 1s–3d intensity is the average for the two irons; therefore, if one assumes that the Fe(III) is unchanged on Rieske-site reduction (1s–3d amplitude remains 26), the Fe(II) must have a 1s–3d amplitude of 10.

There is little published data addressing the question of 1s–3d intensity in Fe(II) complexes. A decrease of ca. 20% in 1s–>3d intensity is predicted for Fe(II) relative to Fe(III) on the basis of a decrease in d vacancies from five to four. Edge spectra for $Fe(S_2\text{-}o\text{-}xyl)_2^{-1/-2}$ show ca. 40% decrease in 1s–3d intensity for Fe(II) vs Fe(III) (Teo & Shulman, 1982); however, McDermott et al. (1988) have questioned the validity of these spectra and reported that there are no significant changes in the XANES on reduction. Even a 40% reduction in 1s–3d intensity would give a predicted intensity of ca. 15 for 4-coordinate Fe(II). This is still significantly larger than the calculated Fe(II) 1s–>3d intensity for reduced PDO.

In order to interpret this result, it is necessary to consider the factors that contribute to the 1s–3d intensity. In general, 1s–3d intensity arises both from direct quadrupole coupling of the 1s and 3d orbitals (Hahn et al., 1982) and from mixing of p-symmetry orbitals (specifically Fe 4p) into the Fe 3d ground state. The quadrupole component is small in comparison with the observed intensity and should be independent of geometry; thus a decrease in the quadrupole component cannot account for the observed intensity reduction. An increase in covalency would decrease the metal contributions to the "3d" ground state, thus reducing the observed 1s–3d intensity; however, electronic structure calculations for Fe_2S_2 clusters (Noodleman & Baerends, 1984; Noodleman et al., 1985) suggest that there is little change in the covalency of the Fe site on reduction. A more likely possibility is that the 4p contribution to the 3d ground state is decreased for the reduced Rieske cluster. This could arise from an increase in coordination number and/or a change in geometry at one of the iron sites.

The ENDOR spectra show that only two nitrogens are coordinated in reduced PDO (Gurbiel et al., 1989); thus if the coordination number does increase, the most likely candidate for an additional ligand is an oxygen either from an amino acid side chain or from the peptide backbone. With regard to the latter possibility, it is interesting to note that there is a conserved loop in the ferredoxin sequences (Matsubata & Hase, 1982), which in the oxidized *Spirulina platensis* ferredoxin structure (Tsukihara et al., 1978) places a carbonyl oxygen from the peptide backbone at ca. 2.8 Å from one Fe. If a similar structure were present in PDO, a carbonyl oxygen could be poised to bind to one of the irons on reduction. Variation in such ligation could conceivably play a role in tuning the reduction potentials of Fe_2S_2 clusters similar to the role proposed for the axial ligands in blue copper proteins (Norris et al., 1986; Gray & Malmstrom, 1983). We emphasize, however, that these interpretations must be regarded as tentative in the absence of XANES data for crystallographically characterized 4- and 5-coordinate Fe(II) models containing both sulfur and nitrogen ligation. Other interpretations, for example, distortion of one of the irons from tetrahedral toward square planar, could also account for the observed decreased in 1s–3d intensity. From the EXAFS results, any such geometrical changes must be accomplished without major changes in bond lengths. Regardless of the interpretation, the XANES data suggest that the structure of the Rieske cluster changes on reduction.

CONCLUSIONS

We find that the Rieske-like cluster has a structure very similar to those found for other [2Fe-2S] clusters, thus demonstrating that the change from thiolate to imidazole ligation has no detectable consequences for Fe_2S_2 core structure. Likewise, changes in the metal occupancy of the mononuclear site and binding of substrate to have no detectable effect on

the structure of the Rieske-like cluster. The mononuclear site makes only a small contribution to the PDO EXAFS, suggesting that this site has predominantly low-Z ligation. Finally, we find that there are unusual features in both the EXAFS and the XANES spectra of reduced PDO that can be interpreted as being consistent with the binding of an additional low-Z ligand to the reduced Rieske cluster, giving one 4-coordinate and one 5-coordinate iron. We plan EXAFS and XANES studies of reduced Fe–S complexes in order to clarify the interpretation of the reduced PDO spectra.

ACKNOWLEDGMENTS

We thank R. A. Scott for the Fe–S model EXAFS data and D. Coucouvanis and A. L. Roe for helpful discussions.

REFERENCES

Antonio, M. R., Averill, B. A., Moura, I., Moura, J. J. G., Orme-Johnson, W. H., Teo, B. K., & Xavier, A. V. (1982) *J. Biol. Chem. 257*, 6646–6649.

Axcell, B. C., & Geary, P. J. (1975) *Biochem. J. 146*, 173–183.

Batie, C. J., LaHaie, E., & Ballou, D. P. (1987) *J. Biol. Chem. 262*, 1510–1518.

Beinert, H., Emptage, M. H., Dreyer, J. C., Scott, R. A., Hahn, J. E., Hodgson, K. O., & Thompson, A. J. (1983) *Proc. Natl. Acad. Sci. U.S.A. 80*, 393–396.

Berg, J. M., & Holm, R. H. (1982) *Met. Ions Biol. 4*, 1–66.

Bowyer, J. R., & Crofts, A. R. (1981) *Biochim. Biophys. Acta 636*, 218–233.

Bunker, B., & Stern, E. A. (1977) *Biophys. J. 19*, 253–264.

Cline, J. F., Hoffman, B. M., LaHaie, E., Ballou, D. P., & Fee, J. A. (1985) *J. Biol. Chem. 260*, 3251–3254.

Coucouvanis, D., Swenson, D., Baenziger, N. C., Holah, D. G., Kostikas, A., Simopoulos, A., & Petrouleas, V. (1976) *J. Am. Chem. Soc. 98*, 5721.

Coucouvanis, D., Swenson, D., Baenziger, N. C., Murphy, C., Holah, D. G., Sfarnas, N., Simopoulos, A., & Kostikas, A. (1981) *J. Am. Chem. Soc. 103*, 3350–3362.

Coucouvanis, D., Salifoglou, A., Kanatzidis, M. G., Simopoulos, A., & Papaefthymious, V. (1984) *J. Am. Chem. Soc. 106*, 6081–6082.

Fee, J. A., Findling, K. L., Yoshida, T., Hille, R., Tarr, G. E., Hearshen, D. O., Dunham, W. R., Day, E. P., Kent, T. A., & Munck, E. (1984) *J. Biol. Chem. 259*, 124–133.

Gabellini, N., Bowyer, J. As., Hurt, E., Melandri, B. A., & Hauska, G. (1982) *Eur. J. Biochem. 126*, 105–111.

Geary, P. J., Saboowalla, F., Patil, D., & Cammack, R. (1984) *Biochem. J. 217*, 667–673.

Gibson, D. T., Hensley, M., Yoshioka, H., & Mabry, T. J. (1970) *Biochemistry 9*, 1626–1630.

Gray, H. B., & Malmstrom, B. G. (1983) *Comments Inorg. Chem. 2*, 203–209.

Gurbiel, R. J., Batie, L. J., Shivaraja, M., True, A. E., Fee, J. A., Hoffman, B. M., & Ballou, D. P. (1989) *Biochemistry 28*, 4861–4871.

Hagen, K. S., Watson, A. D., & Holm, R. H. (1983) *J. Am. Chem. Soc. 105*, 3905.

Hahn, J. E., Scott, R. A., Hodgson, K. O., Doniach, S., Desjardins, S. R., & Solomon, E. I. (1982) *Chem. Phys. Lett. 88*, 595–598.

Hurt, E., & Hauska, G. (1981) *Eur. J. Biochem. 117*, 591–599.

Jinxua, C., & Changneng, C. (1985) *J. Am. Chem. Soc. 99*, 4351–4355.

Koch, S. A., Maelia, L. E., & Millar, M. (1983) *J. Am. Chem. Soc. 105*, 5944–5945.

Kuila, D., & Fee, J. A. (1986) *J. Biol. Chem. 261*, 2768–2771.

Lane, R. W., Ibers, J. A., Frankel, R. B., Papefthymiou, G. C., & Holm, R. H. (1977) *J. Am. Chem. Soc. 99*, 84.

Lindahl, P. A., Teo, B.-K., & Orme-Johnson, W. H. (1987) *Inorg. Chem. 26*, 3912–3916.

MacGillavry, C. H., & Rieck, G. D., Eds. (1985) *International Tables for X-ray Crystallography*, Vol. III, D. Reidel, Boston, pp 171–174.

Maelia, L. E., & Koch, S. A. (1986) *Inorg. Chem. 25*, 1896–1904.

Matsubara, H., & Hase, T. (1982) in *Protein and Nucleic Acids in Plant Systematics* (Jensen, U., & Fairbrothers, D. E., Eds.) Springer-Verlag, Berlin, p 168.

Mayerle, J. J., Denmark, S. E., DePamphilis, B. V., Ibers, J. A., & Holm, R. H. (1975) *J. Am. Chem. Soc. 97*, 1032.

McDermott, A. E., Yachandra, V. K., Guiles, R. D., Britt, R. D., Dexheimer, S. L., Sauer, K., & Klein, M. P. (1988) *Biochemistry 27*, 4013–4020.

Millar, M., Lee, J. F., Koch, S. A., & Fikar, R. (1982) *Inorg. Chem. 21*, 4105.

Nelson, N., & Newmann, J. (1972) *J. Biol. Chem. 247*, 1817–1824.

Noodleman, L., & Baerends, E. J. (1984) *J. Am. Chem. Soc. 106*, 2316–2327.

Noodleman, L., Norman, J. G., Jr., Osborne, J. H., Aizman, A., & Case, D. A. (1985) *J. Am. Chem. Soc. 107*, 3418–3426.

Norris, G. E., Anderson, B. F., & Baker, E. N. (1986) *J. Am. Chem. Soc. 108*, 2784–2785.

Penner-Hahn, J. E., Tsang, H.-T., Batie, C. J., & Ballou, D. P. (1987) *Recl. Trav. Chim. Pays-Bas 106*, 228.

Rieske, J. S., Hansen, R. E., & Zaugg, W. S. (1964) *J. Biol. Chem. 239*, 3017.

Roe, A. L., Scheider, D. J., Mayer, R. J., Pyrz, J. W., Widom, J., & Que, L., Jr. (1984) *J. Am. Chem. Soc. 106*, 1676–1681.

Sauber, K., Frohner, C., Rosenberg, G., Eberspacher, J., & Lingens, F. (1977) *Eur. J. Biochem. 74*, 89–97.

Sayers, D. E., Lytle, F. W., & Stern, E. A. (1971) *Phys. Rev. Lett. 27*, 1204.

Sayers, D. E., Stern, E. A., & Herriott, J. R. (1976) *J. Chem. Phys. 64*, 427–428.

Shulman, R. G., Eisenberger, P., Blumberg, W. E., & Stombaugh, N. A. (1975) *Proc. Natl. Acad. Sci. U.S.A. 72*, 4003–4007.

Shulman, R. G., Yafet, Y., Eisenberger, P., & Blumberg, W. E. (1976) *Proc. Natl. Acad. Sci. U.S.A. 98*, 1384–1388.

Shulman, R. G., Eisenberger, P., Teo, B.-K., Kincaid, B. M., & Brown, G. S. (1978) *J. Mol. Biol. 124*, 305–321.

Stephens, P. J., Morgan, T. V., Devlin, F., Penner-Hahn, J. E., Hodgson, K. O., Scott, R. A., Stout, C. D., & Burgess, B. K. (1985) *Proc. Natl. Acad. Sci. U.S.A. 82*, 5661–5665.

Stern, E. A., Heald, S. M. (1979) *Rev. Sci. Instrum. 50*, 1579.

Teo, B.-K., & Lee, P. A. (1979) *J. Am. Chem. Soc. 101*, 2815–2832.

Teo, B.-K., & Shulman, R. G. (1982) *Met. Ions Biol. 4*, 343–366.

Teo, B.-K., Shulman, R. G., Brown, G. S., & Meixner, A. E. (1979) *J. Am. Chem. Soc. 101*, 5624–5631.

Teo, B.-K., Antonio, M. R., & Averill, B. A. (1983) *J. Am. Chem. Soc. 105*, 3751–3762.

Tsukihara, T., Fukuyama, K., Tahara, H., Katsube, Y., Matsuura, Y., Tanaka, N., Kakudo, M., Wada, K., & Matsubara, H. (1978) *J. Biochem. 84*, 1645.

Watenpaugh, K. D., Sieker, L. C., & Jensen, L. H. (1980) *J. Mol. Biol. 122*, 175.